Int. J. High Technology Ceramics **2** (1986) 291–307

Synthesis and Hot-pressing of Single-phase ZrC_xO_y and Two-phase ZrC_xO_y–ZrO_2 Materials

P. Barnier and F. Thévenot

Ecole Nationale Supérieure des Mines de Saint-Etienne Équipe 'Céramiques Spéciales' and Centre de Recherches Rhône-Alpes des Céramiques Spéciales (CRRACS), 158 Cours Fauriel, F 42023 Saint-Etienne Cédex 2, France

SUMMARY

Single-phase zirconium oxycarbide and a two-phase material, zirconium oxycarbide–zirconia, were synthesized by the reaction between zirconium carbide and zirconia powders at 2000°C under vacuum (4 Pa). ZrC_xO_y has the same cubic face centered (c.f.c.) crystallographic structure as zirconium carbide. The insertion of O increases the metal–non-metal bond strength and causes a decrease of the lattice parameter. $ZrC_{0.64}O_{0.26}$ with a = 4·66 Å is the composition of zirconium oxycarbide at the phase boundary with free zirconium dioxide.

The sinterability of these new materials was studied by hot-pressing under argon. Dense specimens without change of composition were obtained after hot-pressing. The hot-pressing temperature necessary to reach a relative density of 0·97 in 1 h was more than 300°C lower (at 1765°C) for zirconium oxycarbide saturated with oxygen than for zirconium carbide. Likewise, an increasing amount of ZrO_2 in the two-phase materials permitted a decrease of the hot-pressing temperature: between 0 and 17 mass% of ZrO_2 the hot-pressing temperature required decreased by more than 200 to 1550°C.

1. INTRODUCTION

Authors[1,2] who have studied the transition-metal carbides of the fourth, fifth and sixth groups of the periodic table have noticed the difficulty of producing these materials without the presence of dissolved oxygen. Zirconium carbide especially[3] shows a great affinity for oxygen. Several

Int. J. High Technology Ceramics 0267-3762/86/$03·50

investigations have been carried out on the reaction between zirconium dioxide and carbon,[4-10] and between zirconium oxide and zirconium carbide.[11-14] Different authors give a partial phase diagram for the Zr–O–C system[15-19] with a homogeneity range of the zirconium oxycarbide phase. However, these studies led to different or contradictory results; this can be explained by the different experimental conditions concerning temperature and atmosphere (argon, vacuum, partial pressure of carbon monoxide). Certain authors conclude that zirconium oxycarbide is unstable,[12,13] whereas Ogawa[20] affirms that the oxycarbides, i.e. the carbides containing dissolved oxygen, of the group IV and actinide elements are so stable that it is hard to obtain the oxygen-free carbides. The most complete study was carried out by Ouensanga and Dodé,[19] who give a phase diagram for the Zr–O–C system at 1555°C.

Until now workers have been interested primarily in the chemical and thermodynamic aspect of the formation of zirconium oxycarbide. We have been interested in the preparation of dense specimens in order to study their properties. Thus, the main aim of this work was the synthesis of powders of single-phase zirconium oxycarbide, and of two-phase material, zirconium oxycarbide–zirconia, by reaction between zirconium dioxide and zirconium carbide at 2000°C under vacuum, and the study of their sinterability by hot-pressing.

These materials had previously never been studied in a densified form and their mechanical properties in particular were unknown. Several possible applications exist: zirconium oxycarbide can be of value as a material for structural applications at very high temperature, or as a component in cemented carbides. If toughening of zirconium oxycarbide by zirconia is induced, the two-phase material could find cutting tool applications.

2. STUDY OF THE REACTION BETWEEN ZrO_2 AND ZrC

2.1. Starting materials

Zirconium carbide (ZrC) powder of high purity was supplied by H. C. Starck ('vacuum quality', low Hf content). The amounts of the principal impurities are in mass%: Fe = 0·012, O = 0·106 and N = 0·253. The formula determined by chemical analysis is $ZrC_{0.963}$. The BET specific surface area was $0{\cdot}5\,m^2\,g^{-1}$. Zirconium dioxide (ZrO_2) powder without stabilizer was supplied by Criceram (UPH V). The specific surface area of this powder was $6{\cdot}6\,m^2\,g^{-1}$. X-ray diffraction analysis showed the presence of both monoclinic and tetragonal zirconium dioxide.

2.2. Procedure

The reaction was studied at 2000°C under a steady-state vacuum of 4 Pa ($\simeq 3 \times 10^{-2}$ torr). Mixtures of ZrO_2 and ZrC powders with the different compositions (molar basis) $ZrO_2 + \alpha ZrC$, with $\alpha = 19, 8, 6, 4, 3{\cdot}25, 2{\cdot}5, 2$, were intimately mixed in ethanol using a 'Turrax' turbine and dried under vacuum at 110°C. Cylindrical specimens (diameter = 20 mm, height $\simeq$ 15 mm) were obtained by uniaxial cold-pressing. Reaction was allowed to proceed at 2000°C for 4 h: this time was sufficient to reach the thermodynamic equilibrium (longer annealing at 2000°C did not change the composition) except for the mixture $ZrO_2 + 19ZrC$. This material therefore was re-milled, cold-pressed and heated again at 2000°C for 4 h in order to achieve complete reaction. After annealing, specimens were crushed in a steel mortar for X-ray diffraction and chemical analysis.

The main elements zirconium, carbon and oxygen were analysed. Zr was determined by combustion of the powder at 1000°C in air for 1 h. After oxidation, only zirconium dioxide remains; hence it is possible to determine the Zr content. To determine the carbon content, the powder was combusted at 1600°C in a 'LECO 523' with the aid of fluxes, and the amount of carbon monoxide was determined using conductimetry. Oxygen was assumed to account for the residual mass.

The amount of zirconium dioxide in the two-phase powders (ZrC_xO_y–ZrO_2) was obtained by quantitative X-ray analysis. After crushing, ZrO_2 was entirely monoclinic. For low contents (<10 mass%), ZrO_2 was determined by extrapolation to the origin of the straight line, $I_{11\bar{1}}ZrO_2/I_{111}ZrC_xO_y$, versus content of added ZrO_2 in the powder to be analysed, with

$I_{11\bar{1}}ZrO_2$: intensity of the principal diffraction peak ($11\bar{1}$) of monoclinic ZrO_2

$I_{111}ZrC_xO_y$: intensity of the principal diffraction peak (111) of ZrC_xO_y

Monoclinic zirconium dioxide supplied by Magnesium Elektron was used for additions. For high contents (>10 mass%), ZrO_2 was obtained from a standard curve plotting $I_{11\bar{1}}ZrO_2/I_{111}ZrC_xO_y$ versus content of ZrO_2 additions to pure ZrC_xO_y.

2.3. Theoretical study of the reaction

For starting mixtures rich in zirconium carbide, the reaction can be written as follows:

$$ZrO_2 + \alpha ZrC \rightarrow (1 + \alpha)ZrC_xO_y + XCO \quad (1)$$

(to simplify, it is assumed that zirconium carbide is stoichiometric).

Considering the reaction equilibrium, the following relations are derived from (1):

$$x = \frac{\alpha - X}{1 + \alpha} \tag{2}$$

$$y = \frac{2 - X}{1 + \alpha} \tag{3}$$

X can be determined by measuring the mass loss of the specimen during reaction (it is supposed that the mass loss is due only to the formation of carbon monoxide). Consequently, the composition of zirconium oxycarbide can be calculated by using the composition of the starting mixture and the measure of the mass loss during reaction.

For the starting mixtures weaker in zirconium carbide, the reaction becomes

$$ZrO_2 + \alpha ZrC \rightarrow (1 + \alpha - A)ZrC_{x_0}O_{y_0} + A\,ZrO_2 + X CO \tag{4}$$

In this case, the zirconium oxycarbide is saturated with oxygen and is therefore in thermodynamic equilibrium with the residual zirconium dioxide. The composition of zirconium oxycarbide at the phase boundary ($A = 0$) is given by the following relations from (2) and (3):

$$x_0 = \frac{\alpha_0 - X_0}{1 + \alpha_0} \tag{5}$$

$$y_0 = \frac{2 - X_0}{1 + \alpha_0} \tag{6}$$

where α_0 is the number of moles of ZrC in the starting mixture to give pure zirconium oxycarbide saturated with oxygen and X_0 is the number of moles of saturated CO formed.

From (5) and (6), the following relation can be written:

$$x_0 - y_0 = \frac{\alpha_0 - 2}{1 + \alpha_0} \tag{7}$$

Considering the reaction equilibrium (4), the following relation is derived:

$$x_0 - y_0 = \frac{\alpha - 2 + 2A}{1 + \alpha - A} \tag{8}$$

From (7) and (8), the number of moles of residual zirconia A is given by the following equation:

$$A = 1 - \frac{\alpha}{\alpha_0}$$

TABLE 1

Composition of ZrC_xO_y and ZrC_xO_y–ZrO_2 in the Reaction Products, According to Chemical X-ray Diffraction Analysis and Calculation from the Weight Loss Measurement During Reaction; Lattice Parameter of Oxycarbide

α	*Starting mixture: mole% ZrC*	*Mass loss/ %*	*Total elemental chemical analysis in*			*X-ray determination: mass% ZrO_2*	$x = \frac{C}{Zr}$	$y = \frac{O}{Zr}$	*x calculated*	*y calculated*	*Mass% ZrO_2 calculated*	*Lattice parameter of ZrC_xO_y/ Å*
			Mass% Zr	*Mass% C*	*Mass% O (by difference)*							
19	95	2·20	89·26	10·32	0·42	0	0·88	0·027	0·87	0·018	—	4·692
8	88·89	2·98	89·14	9·25	1·61	0	0·79	0·10	0·78	0·11	—	4·682
6	85·71	3·54	89·00	8·70	2·30	0	0·74	0·15	0·72	0·15	—	4·677
4	80	4·17	88·76	7·79	3·45	0	0·67	0·22	0·64	0·24	—	4·665
3·25	76·47	5·07	88·25	7·35	4·40	1·8	—	—	—	—	0·8	4·661
2·5	71·43	5·60	87·39	6·79	5·82	7·9	—	—	—	—	8·5	4·660
2	66·67	5·11	86·73	6·32	6·95	13·2	—	—	—	—	15·7	4·659

2.4. Results and discussion

According to the composition of the starting mixture, the solid reaction products, analysed by X-ray diffraction, are only zirconium oxycarbide or a mixture of zirconium oxycarbide and zirconium dioxide (Table 1). ZrC_xO_y has a crystallographic structure which is identical with that of zirconium carbide: c.f.c. (NaCl type). Carbon and oxygen atoms occupy the octahedral interstitial vacancies of the metallic lattice. The zirconium dioxide is entirely in its monoclinic form.

The variation of the lattice parameter of the oxycarbide phase is plotted as a function of the molar content of zirconium carbide in the starting mixture (Fig. 1). Two different domains are observed. On the right side of the figure, we observe a gradual decrease of the lattice parameter with the diminution of the zirconium carbide concentration of the starting mixture. This corresponds to the monophase domain. The lattice parameter decreases with the progressive introduction of oxygen in the metallic lattice. Zirconium oxycarbide is grey-like ZrC, or reddish for specimens rich in oxygen ($x < 0{\cdot}74$ and $y > 0{\cdot}15$).

Below a limiting content of zirconium carbide in the starting material, the lattice parameter of ZrC_xO_y is constant. Two phases are in thermodynamic

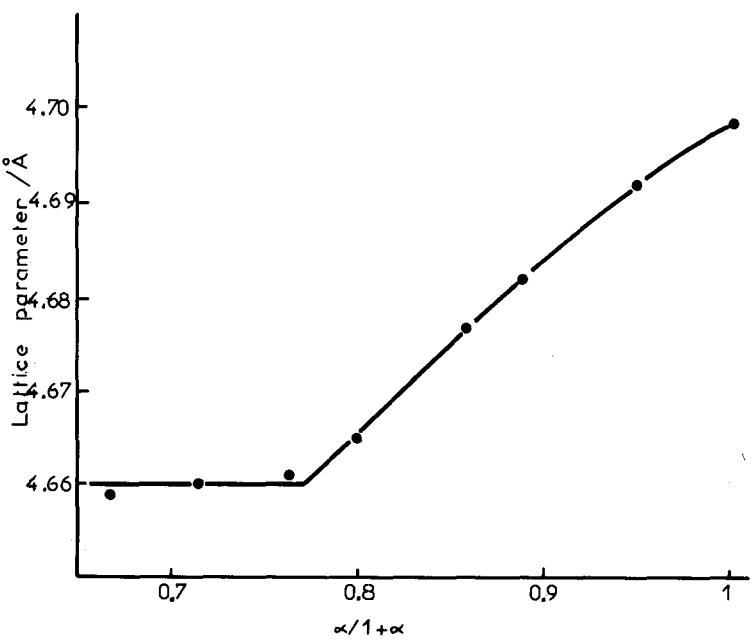

Fig. 1. Variation of the lattice parameter of zirconium oxycarbide after reaction of mixtures ($ZrO_2 + \alpha ZrC$) at 2000°C as a function of the starting molar concentration of zirconium carbide [$\alpha/(1 + \alpha)$].

equilibrium: zirconium oxycarbide saturated with oxygen and zirconium dioxide.

The chemical composition of the specimens is given in Table 1. The amounts of O and C calculated from the weight loss using the relations given above are close to the values obtained by chemical analysis. The phase boundary of the zirconium oxycarbide is obtained for a starting mixture of $ZrO_2 + 3{\cdot}37ZrC$ (see Fig. 1).

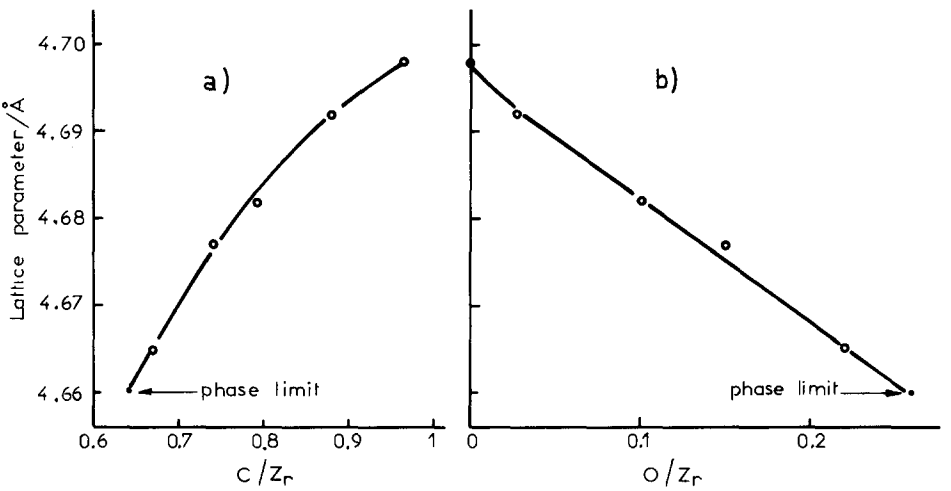

Fig. 2. Variation of the lattice parameter of zirconium oxycarbide as a function of (a) carbon and (b) oxygen concentration.

In Fig. 2 the variation of the lattice parameter of ZrC_xO_y is plotted as a function of the oxygen and carbon content. It can be seen that an increase of the oxygen content or a decrease of the carbon content leads to a decrease of the lattice parameter. The composition of zirconium oxycarbide saturated in oxygen is determined by extrapolation, $ZrC_{0{\cdot}64}O_{0{\cdot}26}$, using the limit parameter 4·66 Å found in Fig. 1. It can be seen that the insertion of oxygen is accompanied by an increase in the concentration of octahedral vacancies ($x + y < 1$ and decreases when y increases). To determine the real influence of oxygen, we compared the variation of the lattice parameter as a function of the occupation of the octahedral vacancies for the oxycarbide phase and for non-stoichiometric zirconium carbide according to Ramqvist[3] (Fig. 3). It can be seen that, in this interval of concentration of octahedral vacancies, the lattice parameter of ZrC_x is almost constant. The lattice parameter of ZrC_xO_y is always less than that of ZrC_x and the difference between the two parameters increases with increasing y. This proves that the Zr–O bond (certainly partially

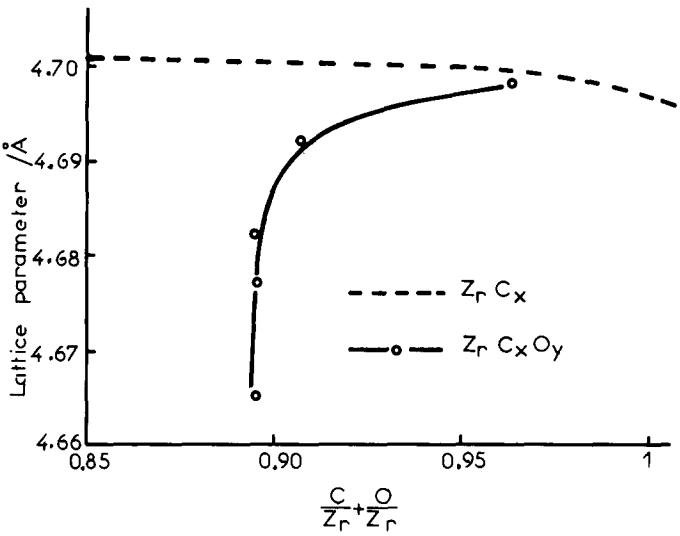

Fig. 3. Comparison of the lattice parameter of the oxycarbide phase and of non-stoichiometric zirconium carbide according to Ramqvist,[3] as a function of the degree of occupation of the octahedral vacancies.

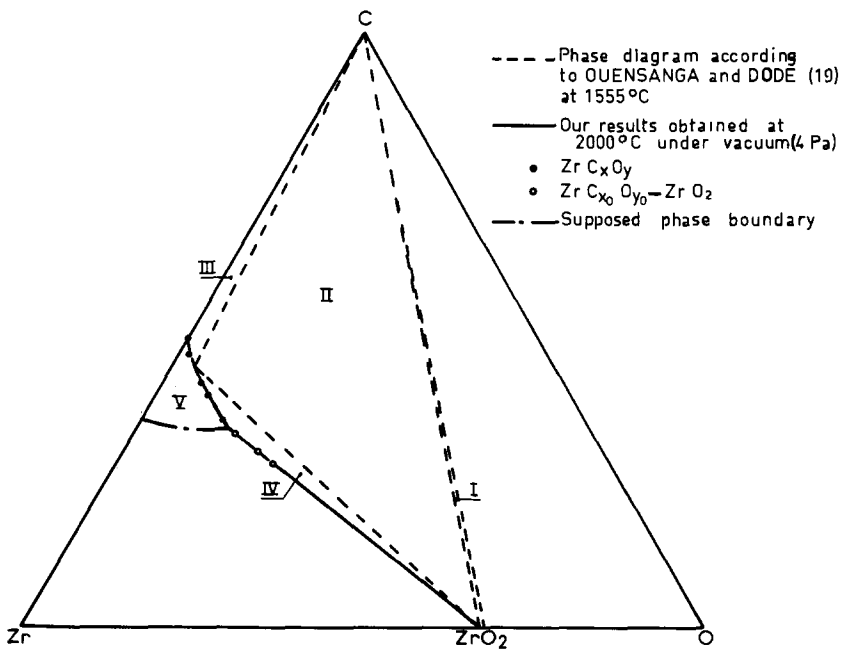

Fig. 4. Results obtained in this study at 2000°C plotted on the Zr–O–C diagram. Diagram given by Ouensanga and Dodé[19] obtained at 1555°C with five domains (I, 'ZrO_2'–C, $P_{CO} > 4 \times 10^4$ Pa (300 torr); II, 'ZrO_2'–C–ZrC_xO_y, $P_{CO} = 4 \times 10^4$ Pa; III, ZrC_xO_y–C, $P_{CO} < 4 \times 10^4$ Pa; IV, ZrC_xO_y–'ZrO_2', $P_{CO} < 4 \times 10^4$ Pa; V, ZrC_xO_y).

ionic) is stronger than the covalent Zr–C bond, and leads to a contraction of the lattice.

The results obtained are plotted in a Zr–O–C diagram (Fig. 4). We also show the results of the work of Ouensanga and Dodé[19] obtained at 1555°C. There is good agreement between the two studies. At 2000°C it is possible to insert more oxygen in the oxycarbide lattice ($ZrC_{0.64}O_{0.26}$) than at 1555°C ($ZrC_{0.73}O_{0.14}$). On the other hand, oxycarbides in the single-phase domain produced by Ouensanga and Dodé at 1555°C under a pressure of 1·3 mPa (10^{-5} torr) (the points are not plotted in Fig. 4) have compositions close to our results obtained at 2000°C under a pressure of 4 Pa (3×10^{-2} torr). The phase boundary (Zr side) of the zirconium oxycarbide domain was supposed to be a line between $ZrC_{0.575}$ (phase boundary of non-stoichiometric zirconium carbide with zirconium according to Ramqvist[3]) and $ZrC_{0.64}O_{0.26}$ (phase boundary of zirconium oxycarbide with zirconium dioxide).

3. HOT-PRESSING OF ZrC_xO_y AND ZrC_xO_y–ZrO_2

3.1. Powder preparation and characterization

After reaction, the specimens were milled in ethanol in a 'Dangoumau' mill, using a stainless steel jar and balls, for 4 h. The contamination by iron was removed by washing in concentrated hydrochloric acid at temperatures between 80°C and boiling point for 0·5 h. The acid, and iron salts, were removed by rinsing with water, followed by acetone, before drying. The operation was repeated twice to ensure the complete elimination of iron. For powders rich in oxygen, a (non-negligible) solution of zirconium oxycarbide was noticed: washing was carried out at 80°C to minimize the solution. For composite powders, the zirconium dioxide content was determined a second time, after washing, by quantitative X-ray diffraction analysis.

The BET specific surface area was measured for all powders (Table 2) and showed values between 0·5 and 1 $m^2 g^{-1}$.

The theoretical density of zirconium oxycarbide was calculated from the chemical analysis and from the determination of the lattice parameter. For two-phase materials, X-ray diffraction analyses of polished specimens show that the zirconium dioxide is certainly entirely monoclinic. Hence, the following relation was used for calculating the theoretical density of the two-phase material:

$$d = \frac{100}{\frac{t}{d_1} + \frac{(100 - t)}{d_2}}$$

TABLE 2

Characterization of the Starting Powders and Results of Hot-pressing of ZrC_xO_y and ZrC_xO_y–ZrO_2

Composition of the starting powder	*Mass% ZrO_2*	*BET specific area/ $m^2 g^{-1}$*	*Lattice parameter of ZrC_xO_y/ Å*	*Theoretical density/ $Mg m^{-3}$*	*Hot-pressing temperature/ °C*	*Sintering time/ h*	*Pressure/ MPa*	*Lattice parameter after hot-pressing/ Å*	*Final density/*		*Hot-pressing temperature required for 0·97 theoretical density (time = 1 h)/ °C*
									$Mg m^{-3}$	*% theoretical density*	
$ZrC_{0·963}$	0	0·5	4·698	6·58	1 900	1	40	4·697	6·07	(92·2)	2 100
					2 000	1	40	4·699	6·35	(96·5)	
					2 100	1	40	4·698	6·38	(97·0)	
					2 200	1	40	—	6·40	(97·3)	
$ZrC_{0·88}O_{0·027}$	0	1	4·692	6·57	1 800	1	32	4·691	5·82	(88·6)	1 915
					1 900	1	32	4·693	6·36	(96·8)	
					1 950	0·75	32	4·690	6·27	(95·4)	
					2 000	1	32	4·692	6·48	(98·6)	
$ZrC_{0·79}O_{0·10}$	0	1	4·682	6·62	1 800	1	32	4·683	6·22	(94·0)	1 870
					1 900	0·5	32	4·682	6·53	(98·6)	
					1 900	1	32	4·683	6·50	(98·2)	
					2 000	0·5	32	4·681	6·44	(97·3)	
					2 000	1	32	4·680	6·55	(98·9)	
$ZrC_{0·74}O_{0·15}$	0	0·6	4·677	6·65	1 800	1	32	4·678	6·39	(96·1)	1 830
					1 850	1	32	4·676	6·49	(97·6)	
					1 900	0·5	32	4·678	6·56	(98·6)	
					1 900	1	32	4·677	6·64	(99·8)	
					2 000	1	32	4·678	6·63	(99·7)	

$ZrC_{0.67}O_{0.22}$	0	0·6	4·665	6·72	1 700	1	32	4·667	6·42	(95·5)	1 765
					1 750	1	32	4·664	6·47	(96·3)	
					1 800	1	32	4·667	6·58	(97·9)	
					1 850	0·75	32	4·666	6·68	(99·4)	
					1 900	0·5	32	4·665	6·71	(99·9)	
					1 900	1	32	4·666	6·72	(100)	
					2 000	1	32	4·663	6·71	(99·9)	
	2·4	0·6	4·661	6·73	1 600	1	32	4·660	6·42	(95·4)	1 625
					1 650	1	32	4·661	6·60	(98·1)	
					1 750	1	32	4·660	6·68	(99·3)	
					1 800	0·5	32	4·660	6·70	(99·6)	
					1 800	1	32	4·665	6·71	(99·7)	
					1 850	1	32	4·663	6·72	(99·9)	
$ZrC_{0.64}O_{0.26}$ + ZrO_2	10·1	0·9	4·660	6·62	1 600	1	32	4·661	6·36	(96·1)	1 640
					1 700	1	32	4·662	6·52	(98·5)	
					1 750	1	32	4·661	6·54	(98·8)	
					1 800	0·5	32	4·663	6·58	(99·4)	
					1 800	1	32	4·664	6·59	(99·5)	
	17·0	0·9	4·559	6·52	1 500	1	32	4·660	6·20	(95·1)	1 550
					1 600	0·5	32	4·661	6·28	(96·3)	
					1 600	1	32	4·661	6·44	(98·8)	
					1 750	1	32	4·662	6·49	(99·5)	

where d is the density of the two-phase material; d_1 is the density of monoclinic zirconium dioxide, $d_1 = 5{\cdot}56\,\mathrm{Mg\,M^{-3}}$; d_2 is the density of zirconium oxycarbide saturated with oxygen, $d_2 = 6{\cdot}76\,\mathrm{Mg\,m^{-3}}$; and t is the mass% of ZrO_2.

3.2. Hot-pressing procedure

The hot-press used has already been described in previous papers.[21-23] Graphite dies and punches were used to obtain cylindrical-shaped specimens 20 mm in diameter and 8 to 12 mm in height after hot-pressing. The hot-pressing results for zirconium carbide are taken from a previous study.[24]

For ZrC_xO_y and ZrC_xO_y–ZrO_2, a chemical barrier is necessary to avoid reaction of the specimen with carbon. The powder is encapsulated in tantalum foil (thickness = 0·025 mm), and is then embedded in hexagonal boron nitride. This method has already been used with success to produce dense boron and boron suboxide.[22,25] During hot-pressing, the temperature was raised linearly with time at 30°C $\mathrm{min^{-1}}$ with a low applied pressure of 8 MPa, under vacuum up to 1000°C and under argon at higher temperature. At its maximum, the temperature was held for 0·5 to 1 h and a pressure of 32 MPa was applied (40 MPa for zirconium carbide). Then the temperature was decreased linearly with time at 30°C $\mathrm{min^{-1}}$ without pressure for ZrC_xO_y and at a speed of 10°C $\mathrm{min^{-1}}$ in the case of ZrO_2-containing material to avoid the formation of macrocracks during the martensitic transformation of zirconium dioxide which involves an increase in volume.

After hot-pressing, the surface of the specimens was polished before measuring the density and before X-ray examination. The lattice parameter of ZrC_xO_y was calculated and compared with the parameter of the initial powder.

3.3. Results and discussion

The results of the hot-pressing experiments are summarized in Table 2. No appreciable change of the lattice parameters of the oxycarbide was observed in the single-phase domain. This proves that the chemical composition of the zirconium oxycarbide phase remains constant and the stability of this phase can be confirmed under the conditions of this investigation. At higher hot-pressing temperatures ($T > 1800$°C), the lattice parameter of zirconium oxycarbide in the two-phase system increased slightly. This can be explained by the slightly different conditions of the thermodynamic equilibrium for the reaction of the powders (vacuum) on the one hand

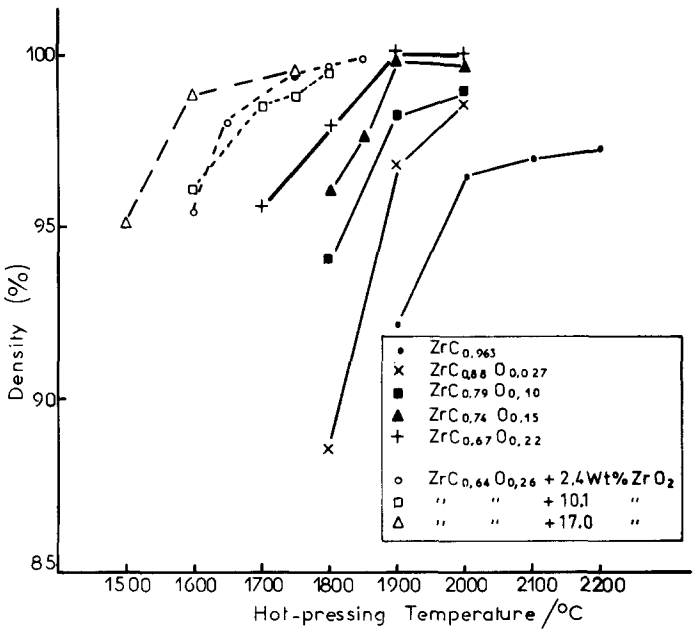

Fig. 5. Variation of the relative density of ZrC_xO_y and ZrC_xO_y–ZrO_2 as a function of the hot-pressing temperature (sintering time = 1 h).

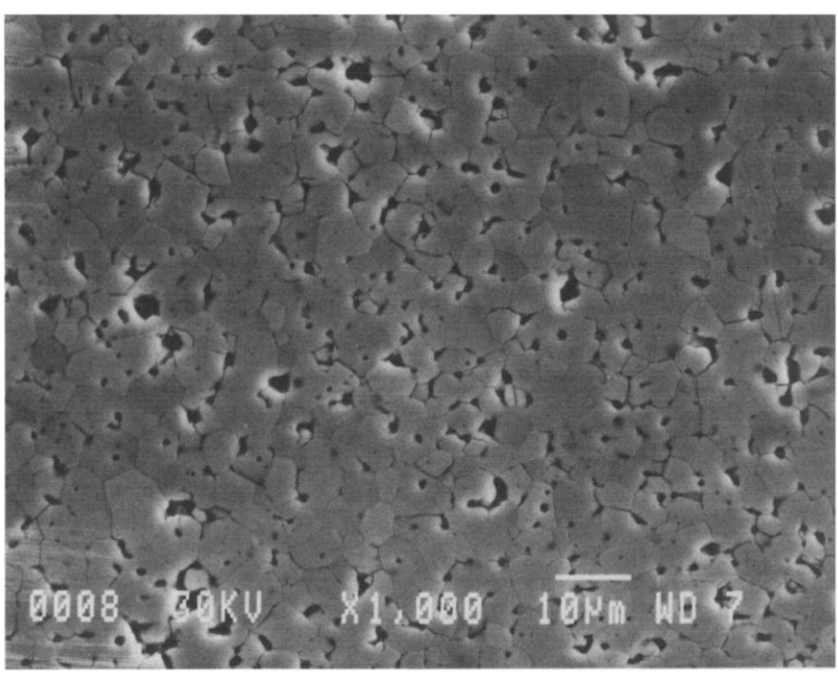

Fig. 6. Scanning electron micrograph of $ZrC_{0{\cdot}74}O_{0{\cdot}15}$ hot-pressed at 1900°C for 30 min, using secondary electrons (chemical etching).

and for hot-pressing (argon atmosphere and application of pressure) on the other hand. At lower temperatures there is no variation of the lattice parameter, since the reaction kinetics is very slow and the reaction equilibrium is metastable.

For all compositions it was possible to obtain specimens of high density. The variation of the relative density with different hot-pressing temperatures is shown in Fig. 5. It can be seen that the sinterability of zirconium oxycarbide increases, when the oxygen content increases. In Table 2 is noted the hot-pressing temperature necessary to reach a relative density of 97% in 1 h: for zirconium oxycarbide rich in oxygen ($ZrC_{0\cdot67}O_{0\cdot22}$), the temperature necessary (1765°C) is 335°C lower than the temperature necessary for zirconium carbide (2100°C). For materials with a low amount of ZrO_2 (2·4 mass%) the hot-pressing temperature necessary to reach a density of 97% is only 1625°C, whereas 1765°C is required for $ZrC_{0\cdot67}O_{0\cdot22}$. Materials with 10·1 mass% of ZrO_2 have a slightly worse sinterability but only 1550°C is necessary to reach a density of 97% for materials with 17·0 mass% of ZrO_2.

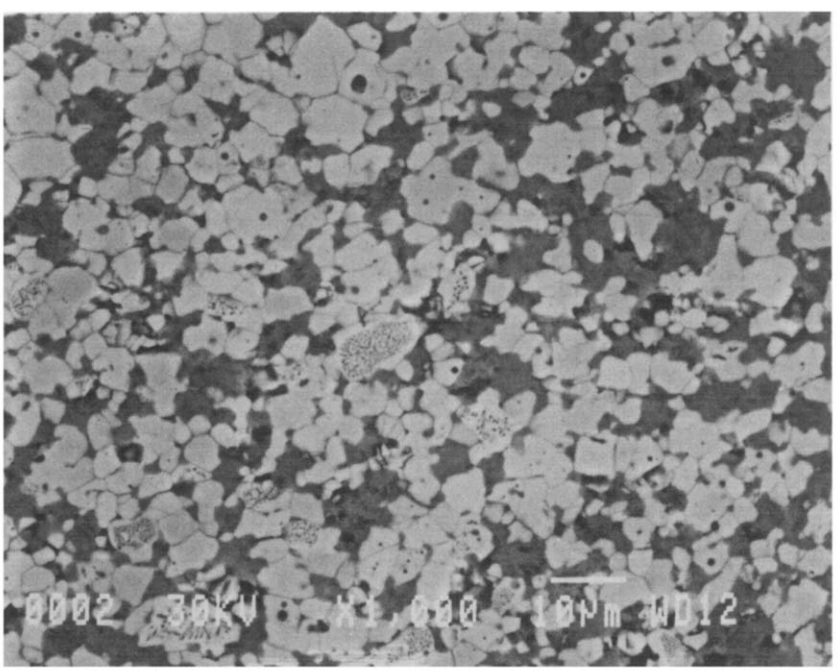

Fig. 7. Scanning electron micrograph of the two-phase material $ZrC_{0\cdot64}O_{0\cdot26}$–17·0 mass% ZrO_2, hot-pressed at 1600°C for 60 min, using back-scattered electrons (without chemical etching; zirconium oxycarbide, zirconium dioxide and porosity appear respectively as light, grey and dark).

Metallographic examinations of polished specimens were made by SEM; Fig. 6 shows the microstructure of $ZrC_{0.74}O_{0.15}$ hot-pressed at 1900°C for 0·5 h. The surface was etched with a solution of nitric and hydrofluoric acids: grain boundaries are well etched but attack by acids increases the size of holes due to porosity or caused by abrasion. Figure 7 shows the microstructure of a two-phase material ($ZrC_{0.64}O_{0.26}$ + 17·0 mass% ZrO_2) hot-pressed at 1600°C for 1 h. Polishing is sufficient to reveal the grain boundaries. The image was taken using back-scattered electrons in order to obtain better phase contrast.

4. CONCLUSION

The synthesis of powders of single-phase ZrC_xO_y and of two-phase ZrC_xO_y–ZrO_2 was achieved by reaction between zirconium carbide and zirconium dioxide powders at 2000°C under vacuum (4 Pa).

The sintering of these new materials has been studied for the first time by hot-pressing under argon. Specimens with good density and without change of composition during hot-pressing were obtained. The sinterability of oxycarbide increased considerably with the oxygen content, and increased still further for materials containing ZrO_2, even when the amount of ZrO_2 was low.

The thermomechanical properties of these new materials will now be investigated. The possibility in particular of toughening zirconium oxycarbide by zirconia will be studied.

REFERENCES

1. Toth, L. E., *Transition Metal Carbides and Nitrides*, Academic Press, New York and London, 1971.
2. Storms, E. K., *The Refractory Carbides*, Academic Press, New York, 1967.
3. Ramqvist, L., Variation of lattice parameter and hardness with carbon content of group 4b metal carbides, *Jerkont. Ann.*, **152** (1968) 517–23.
4. Henney, J. and Jones, J. W. S., Phases in the zirconium–carbon–oxygen system, in *Special Ceramics*, Ed. P. Popper, Academic Press, London, 1964, 35–43.
5. Leprince-Ringuet, F., Contribution à l'étude de l'action du carbone sur les oxydes réfractaires à haute température, *Ann. Chim.*, **2** (1967) 297–306.
6. Ouensanga, A., Vermesse, C. and Dodé, M., Contribution à l'étude thermodynamique du système Zr–O–C à haute température, *Rev. Chim. Miner.*, **9** (1972) 473–81.
7. Ouensanga, A. and Dodé, M., Etude à 1555°C de la solubilité de l'oxygène dans le carbure de zirconium en présence de carbone libre et dans les conditions

d'équilibre thermodynamique, *Rev. Int. Hautes Temp. et Réfract.*, **11** (1974) 35–9.
8. Ouensanga, A., Pialoux, A. and Dodé, M., Etude aux rayons X à haute température du système Zr–O–C dans les conditions d'équilibre thermodynamique, puis sous vide, *Rev. Int. Hautes Temp. et Réfract.*, **11** (1974) 289–93.
9. Kutsev, V. S. and Zhelankin, V. I., Thermodynamics of carbothermal reduction of zirconium and hafnium oxides, *Izv. Akad. Nauk SSSR, Neorg. Mater.*, **14** (1978) 593–5.
10. Lyubimov, V. D., Shveikin, G. P. and Alyamovskii, S. I., Mechanism of the direct reduction of tantalum, hafnium, and zirconium oxides, *Zh. Neorg. Khim.*, **27** (1982) 3015–19.
11. Fedorus, V. B., Kosolapova, T. Ya. and Kuzma, Yu. B., Interaction of carbides of transition metals of groups IV–VI of periodic system of elements with zirconium oxide, *Rev. Int. Hautes Temp. et Réfract.*, **6** (1969) 193–7.
12. Gropyanov, V. M., Kovaleskaya, T. A. and Yudin, B. F., Stability of oxycarbides in the system ZrC–ZrO_2, *Izv. Akad. Nauk SSSR, Neorg. Mater.*, **8** (1972) 88–91.
13. Gropyanov, V. P., Kovalevskaya, T. A. and Razumovskii, S. N., Crystal structure of zirconium oxycarbides in the system ZrC–ZrO_2, *Izv. Akad. Nauk SSSR, Neorg. Mater.*, **8** (1972) 92–5.
14. Granov, V. I. and Glaskov, A. V., Theoretical analysis of the reaction of zirconium dioxide with zirconium carbide, *Izv. Akad. Nauk SSSR, Neorg. Mater.*, **11** (1975) 226–9.
15. Alyamovskii, S. I., Zainulin, Yu. G., Schveikin, G. P. and Gel'd, P. V., Concentration range corresponding to the stability of the cubic (NaCl type) zirconium oxide carbide and the degree of filling of its unit cell, *Zh. Neorg. Khim.*, **6** (1971) 7–11.
16. Klimashin, G. M., Kozlovskii, L. V. and Chiu, A. K., Region of existence of an oxycarbide phase in the system Zr–C–O, *Zh. Prikl. Khim.*, **44** (1971) 1644–6.
17. Klimashin, G. M., Avgustinik, A. I. and Smirnov, G. V., Carbonitride and oxycarbide phases of titanium and zirconium, *Izv. Akad. Nauk SSSR, Neorg. Mater.*, **8** (1972) 843–5.
18. Constant, K., Kieffer, R. and Ettmayer, P., Über des pseudoternäre System 'ZrO'–ZrN–ZrC, *Monatsh. Chem.*, **106** (1975) 823–32.
19. Ouensanga, A. H. and Dodé, M., Etude thermodynamique et structurale à haute température dy système Zr–C–O. Diagramme de phases à 1555°C, *J. Nucl. Mater.*, **59** (1976) 49–60.
20. Ogawa, T., Method to assess the equilibrium MO_x–'MC_y'–C–CO. The system ZrO_2–'ZrC'–C–CO, *J. Chem. Eng. Data*, **27** (1982) 186–8.
21. Brodhag, C. and Thévenot, F., Utilisation d'un système de traitement informatique interactif APL pour le suivi de la fabrication de pièces frittées par compression à chaud, in *Proc. Colloque sur le Contrôle de Qualité et l'Assurance de la Qualité en Métallurgie des Poudres*, Société Française de Métallurgie, Paris, September 1980, Vol. 10, 1–6.
22. Brodhag, C., *Etudes sur le Bore et les Composés Interstitiels du Bore Alpha—Traitement Infographique des Cinétiques de Frittage sous Charge*, Thesis, University of Limoges, France, 1983.

23. Brodhag, C., Bouchacourt, M. and Thévenot, F., La cinétique de la compression à chaud de céramiques spéciales, *Silicates Ind.*, **4–5** (1981) 91–101.
24. Barnier, P., Brodhag, C. and Thévenot, F., Hot-pressing kinetics of zirconium carbide, *J. Mat. Sci.*, **21** (1986) 2547–52.
25. Bouchacourt, M., Brodhag, C. and Thévenot, F., The hot pressing of boron and boron rich compounds, *Science of Ceramics 11*, Stenungsund, Sweden, 14–17 June, 1981, 231–6.

Received 14 February 1986; revised version received 14 July 1986; accepted 3 August 1986